

Three Dimensional Segmentation of Intravascular Ultrasound Data*

Marc Wennogle¹ and William Hoff²

¹Veran Medical Technologies, Nashville, Tennessee
marc.wennogle@veranmedical.com

²Colorado School of Mines, Golden, Colorado
whoff@mines.edu

Abstract. Intravascular ultrasound (IVUS) is a useful imaging technique that can be used to assess the health of coronary arteries. However, manual segmentation of the lumen and adventia boundaries is a time consuming process. Automated methods are needed, but they have to be able to overcome poor signal-to-noise ratios and artifacts commonly present in IVUS images. In this work, three improvements to previous methods were developed and evaluated. These were: (1) a preprocessing step to remove motion artifacts, (2) a new directional gradient velocity term, and (3) a post-processing level-set method. Two IVUS cardiac datasets were used to evaluate the accuracy of the new method over the 3D gradient fast marching method. The new methods, both individually and in combination, were found to significantly lower the volume error.

Keywords: Biomedical imaging, IVUS, ultrasound, segmentation.

1 Introduction

Intravascular ultrasound (IVUS) is a medical imaging technique using a specially designed catheter with a miniaturized ultrasound probe. It can be used in coronary arteries to determine the amount of plaque built up at any particular point, as well as the degree of narrowing of the lumen (the channel in which the blood flows). Hundreds of cross-sectional images are created by advancing the catheter through the blood vessel in a living individual. IVUS can provide three dimensional information on the structure of the artery, including plaque.

Two anatomic contours are of interest in IVUS images (Fig 1). The lumen contour is the border between the dark colored (echolucent) lumen and the light colored (echogenic) inner layer of the vessel wall (intima). In vessels that contain plaque, the lumen contour is the border between the blood and the plaque. The adventitia contour is the boundary between the vessel media and the outer vessel wall (adventitia). The difference between the lumen and adventitia contours can be used to measure the plaque volume.

* The authors gratefully acknowledge the assistance of Dr. James Chen and Dr. John Carroll of the Cardiology Department at the U. of Colorado at Denver and Health Sciences Center.

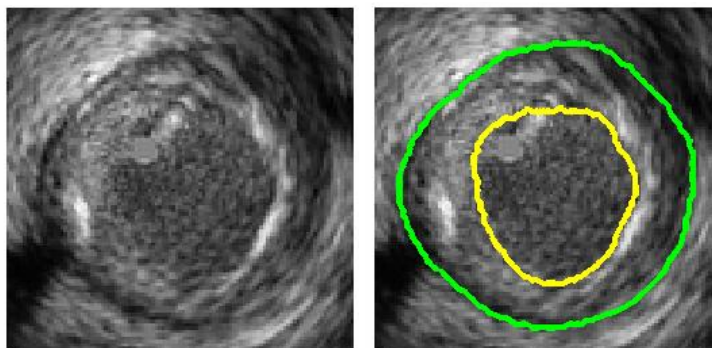


Fig. 1. IVUS cross sectional image: (Left) raw data obtained from the IVUS instrument; (right) superimposed lumen contour (inner) and adventitia contour (outer)

Automated segmentation would be a powerful tool for clinical and research applications, due to the large number of images obtained in an IVUS procedure. Numerous semi-automated segmentation methods have been tested on IVUS data, but some manual intervention is still needed because of the low signal-to-noise ratio and image artifacts in IVUS data. Artifacts include shadowing due to the guide-wire that is next to the transducer, or by a region of highly calcified plaque. Both reflect nearly all the energy of the acoustic signal, causing a shadow behind the obstruction.

A number of methods have been explored for IVUS segmentation. One is the 3D active surfaces method [1-4], which represents the surface of the boundary in the form of a deformable model. The model is initialized by manually placing a contour near the desired contour on each IVUS image. This surface then deformed by external and internal forces, which push or pull the contour until a minimum energy is achieved [5]. The internal forces control the overall shape and continuity of the surface, while the external forces attract the surface to gradient edges of the image. Due to the round geometry of the vessel, a curvature (internal force) term is a desirable characteristic when segmenting IVUS data. The initial surface must be placed close enough to the desired solution or else unwanted convergence will occur.

Rather than drawing an initial contour in each cross sectional image, it can be more efficient to trace the initial surface in a longitudinal view (L-view) representation. The L-view is created by stacking the sequential cross sectional images to form a 3D volume, and then slicing the volume along a plane parallel to the direction of travel (Fig 2(a)). The user can manually trace the contour of interest in a few longitudinal views derived from cutting planes at different angles. The complete contour in each cross sectional image can then be interpolated from the designated points.

Another method used in IVUS segmentation is the 3D fast marching method. Similar to the active surface method, this requires the user to designate the initial surface; however, it has been shown to be less sensitive to the initial placement than the active surface method [6-7]. The fast-marching method is essentially a region growing method, in which the boundary of the region propagates outward using a speed function that is dependent on the magnitude of the local image gradient. The function is designed so that the speed value is near zero at image boundaries, where

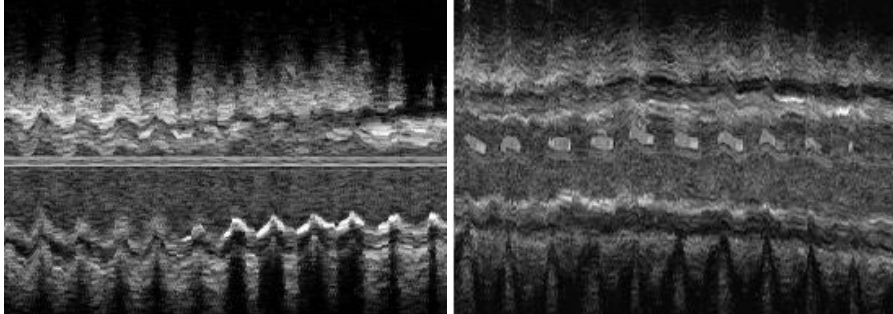


Fig. 2. (a) An L-view slice of a series of IVUS images. The “saw-tooth” appearance is a motion artifact caused by the cardiac cycle of the patient. (b) After removal of the motion artifact.

the gradient magnitude is high. To locate an image boundary of interest, one contour is initialized inside the boundary and another initialized outside the boundary. The contours propagate in opposite directions until they meet in the middle.

The 2D contours actually represent slices of a three dimensional object that is smooth and continuous. Thus, knowledge about the location of the contour in one image can constrain the possible locations of the contour in the adjacent images. For example, information from neighboring images can help overcome noise spikes or shadowing events that occur on a 2D image.

In this paper, we describe an algorithm for IVUS segmentation based on the 3D fast marching method, but with three innovations: (1) We first register the images to reduce the motion artifact, before segmentation, in order to reduce the effort to provide an initial surface. (2) We use a directional gradient term in the speed function of the fast marching method, instead of the gradient magnitude, which takes advantage of the tissue properties of the lumen, media, and adventitia. (3) We post-process the results of the fast marching with a level-set method, that can enforce smoothness constraints. The benefits of these innovations were evaluated by comparing the results to ground truth segmentation of *in vivo* data.

2 Algorithm Description

The 3D fast marching method described by [7] was implemented and used as the basis for IVUS segmentation because of its good performance. This section describes the additional algorithms and innovations that were developed.

2.1 Motion Artifact Removal

We developed a method to register images to remove the motion artifact. The approach uses the method of phase correlation [8], which uses the principle that two images that contain rigid motion (translation and rotation) relative to each other will have a phase shift in their Fourier coefficients. If f_1 and f_2 are consecutive IVUS images that differ only by a translation, then their Fourier transforms are related by $F_2(\omega_x, \omega_y) = F_1(\omega_x, \omega_y) \exp(-i2\pi(\omega_x\tau_x + \omega_y\tau_y))$. Estimation of the phase shift is

found by fitting a regression plane to the phases of the principal frequencies. A rigid translation can be found by applying the method in Cartesian coordinates, while a rigid rotation can be found by applying the method in polar coordinates. A rigid rotation in polar coordinates will appear as a horizontal displacement. The method is first applied in Cartesian coordinates and then polar coordinates to find the translation and rotation between two images. This rigid motion can be removed, thus approximately aligning the two consecutive images (Figure 2(b)).

2.2 Directional Gradient

The fast marching method starts with a manually specified surface at the initial time, $T=0$. It then solves for the arrival time $T(x,y,z)$ of the evolving surface at each point, using the equation $|\nabla T|F = 1$, where F is the speed function and is given by

$$F = \frac{1}{1 + |\nabla G_\sigma * I(x, y, z)|} \tag{1}$$

Here, $G_\sigma * I(x, y, z)$ is the convolution of the image with a Gaussian smoothing filter of width σ . At the location of large gradients, the speed will be close to zero.

However, this speed function does not take advantage of knowledge of the direction of the gradient that occurs in the contours of interest. Because of tissue properties, the lumen and adventitia borders will both appear as transitions from a dark (echolucent) region to a bright (echogenic) region, when traveling radially outward from the center of the image. Thus, the direction of the gradient should point radially outwards at those contours. We can define a speed function that uses a directional gradient term:

$$F = \frac{1}{1 + \left| \max\left(\frac{d}{dr} G_\sigma * I(x, y, z), 0\right) \right|} \tag{2}$$

This function will only accept positive gradients along the radial direction. Figure 3 shows a comparison between the non-directional gradient speed term and the new directional gradient speed term on an example image.

The two dark rings in Figure 3 (right) represent slow velocities and are correctly located on the lumen and adventitia contours. Thus, the fast marching method is more likely to find the contours in the correct place. The non-directional speed function, however, has many more dark areas (low velocities), meaning that the fast marching method may get stuck in an incorrect location.

2.3 Level Set Method

An alternative approach to image segmentation is the level set method, introduced in [9]. This method has been used successfully in medical imaging applications, such as computer-aided cytology [10], although it has not yet been applied to IVUS. In this method, the propagating contour is the zero level set of a time-dependent, implicit function $\phi(\vec{x}, t)$. We initialize $\phi(\vec{x}, t=0) = \pm d$ where $\pm d$ is the signed distance to the initial contour. Taking the derivative with respect to time, we get

$$\phi_t + \frac{\partial \bar{x}}{\partial t} \cdot \nabla \phi = 0 \quad (4)$$

or equivalently

$$\phi_t + J|\nabla \phi| = 0 \quad (5)$$

where J is the speed normal to the level set. The speed function J can be made a function of the curvature of the interface and image characteristics such as edges [11].

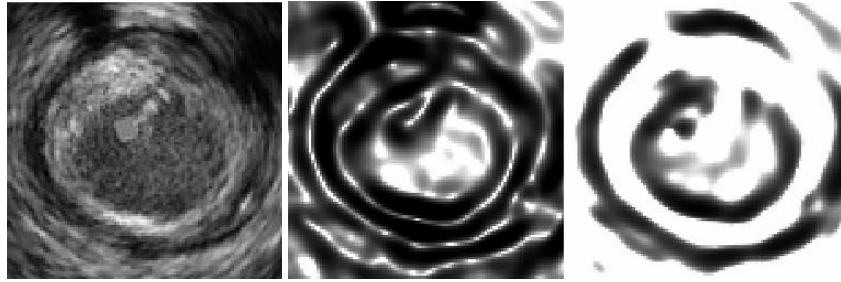


Fig. 3. (Left) IVUS image. (Center) Speed function calculated with the non-directional gradient term. (Right) Speed function calculated with the new directional gradient term.

Unlike the fast marching method where the interface is only allowed to propagate in one direction (forward), the level-set method allows for forward and backward motion. This increases computational complexity, although the efficiency can be improved using a “narrow band” approach, in which computation is only performed on grid points in a narrow band around the zero level-set.

Another gain in efficiency can be achieved by using the level-set method as a post-processing step to another segmentation algorithm, such as the fast marching method [9]. In this technique, the initial location of the interface in the level-set method is the final location of the interface found by the fast marching method. The initial contour should be very close to the desired location, thus minimizing the number of required iterations. We used 60 iterations, with a re-initialization of the level set every 20 iterations. The iteration limit and re-initialization were found empirically to be good parameters that allowed the interface to reach a stable solution.

In this work, we used the formulation of [10] for the level set equation:

$$\phi_t - \varepsilon F \kappa |\nabla \phi| - \beta \nabla P \cdot \nabla \phi = 0 \quad (6)$$

Here, the speed term is $J = \varepsilon F \kappa$ where F is the gradient function and κ is the mean curvature of the surface. The additional term, $\beta \nabla P \cdot \nabla \phi$, is designed to force the surface towards boundaries. The variable P is found by applying a Gaussian smoothing filter to the image gray levels with $P = -|\nabla(G_\sigma * I(i, j, k))|$. The variables ε and β are constants that control the relative strengths of the two terms.

Figure 4 shows a comparison of the results of the fast marching method only, with the results of the combined method (i.e., fast marching method followed by level set method). The contour found by the fast marching method is shown in (a) and the

contour found by subsequent post-processing by the level-set method is shown in yellow. Figure 4 (c) shows both contours for comparison purposes. In many places the contours found by the combined method are closer to the true lumen and adventitia contours than the contours found by the fast marching method.

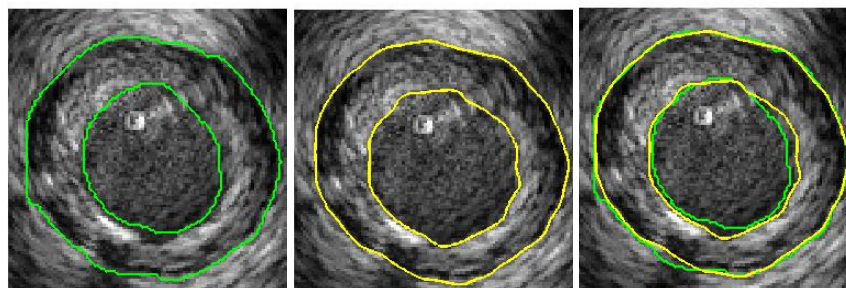


Fig. 4. (a) Solution of the fast marching method for the lumen and adventitia contour; (b) solution of the level-set method; (c) both solutions

3 Experimental Evaluation

The IVUS data used in this research were supplied by the University of Colorado at Denver and Health Sciences Center. Two datasets were taken with a Boston Scientific Galaxy IVUS system at a pull back rate of 0.5 mm/s and a frame rate of 30 rev/s. The first dataset consisted of 290 consecutive IVUS images, each 256x256 pixels, representing approximately 4.8 mm of vessel. The second dataset consisted of 301 consecutive images representing approximately 5.2 mm of vessel.

Evaluations of the segmentation methods were made by comparing computer segmented contours to hand picked contours of the lumen and adventitia borders. The hand picked contours were performed using the Mimics software package, from Materialise Inc. Hand picked contours were made on all images, and were verified by two cardiologists. Any misplaced contours were adjusted during the meetings with the cardiologists. These hand picked contours are considered to be the “ground truth” in this research. The cardiologists stated that the adventitia contour on dataset 2 was too poorly defined and subjective, due to shadow artifacts, to use in this study. Therefore, only the lumen contour of dataset 2 was used in this study.

Area and volume measurements have been widely used to evaluate the plaque volume on IVUS sequences. The summation of the segmented area of each IVUS image in a sequence gives the segmented volume of the vessel. To compare ground truth with the results of the algorithm we computed the non-overlapping volume. The non-overlapping volume was obtained by taking the union of the two volumes and subtracting their intersection [3].

This criterion was used to evaluate the benefit of the phase correlation method, the directional gradient speed term for the 3D gradient fast marching method, and the post fast marching level-set method. Evaluations were compared to the 3D gradient fast marching method as used by [6-7] for IVUS segmentation. A 15x15 pixel

Gaussian smoothing filter of standard deviation $\sigma = 5$ was used in the speed term (these filter parameters were chosen empirically).

Initial contours were manually placed using four L-view slices at equally spaced angles over 360 degrees. The user picked a small set of points along the lumen and adventitia contours, and a smooth curve was interpolated between the points as shown in Figure 5(a). Once the four L-view slices have been picked by a user, each image contains eight picked points on both the lumen and adventitia contours. These points were then spline-interpolated in the image direction and in the direction parallel to the vessel to obtain two closed contours on the lumen and adventitia borders.

An initial inner and outer surface is created by expanding outward and contracting inward the initial manually picked surface described above. If the initial interface is near the desired border, then the two interfaces surround the desired edge. Figure 5(b) shows an example of the initial interface (red) around the adventitia contour and the corresponding contracted and expanded interfaces needed for the multiple interface fast marching method (yellow).

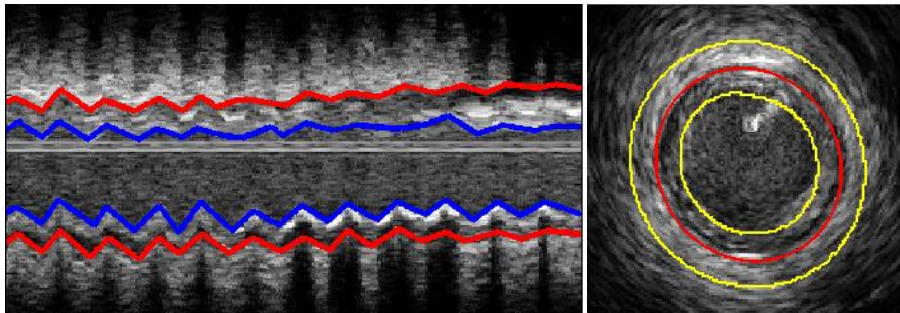


Fig. 5. (a) An L-view slice with the hand picked lumen and adventitia contours. This was from the non-motion compensated dataset and the saw-tooth appearance due to the motion artifact can be seen. (b) A cross-sectional IVUS image with the initial hand picked contour in the middle and two contours created by contracting and expanding the initial contour.

The first experiment evaluated whether removing the motion artifact would improve the accuracy of the fast marching method. Dataset 1 was used in this test because it contained a noticeable motion artifact. The number of initial picks on each L-view contour was restricted to every 50th image. Overall, the non-overlapping volume decreased from 14.3% to 7.6% of the lumen volume and 8.4% to 5.5% of the adventitia volume.

The effect of the number of initial picks on each L-view contour was also evaluated (Figure 6). The x-axis in these figures is the increment of picks (N) on the L-view slices that are needed to produce an initial surface. As the figures show, the results from the motion corrected dataset are more accurate in terms of the percentage of non-overlapping volume.

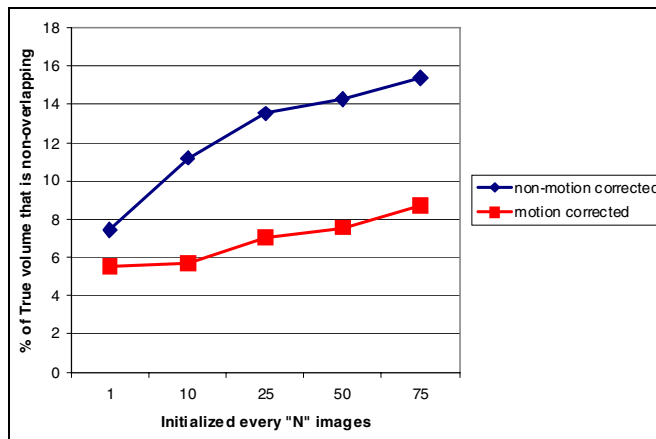


Fig. 6. The results from the phase correlation method on the non-motion corrected and motion corrected dataset #1 for the lumen

The next test performed was to evaluate the benefit of the new directional gradient speed term in the fast marching method. Dataset #1 was used, with motion correction. Use of this term resulted in an improvement of the non-overlapping volume from 11.0% to 7.9% of the lumen volume and 8.6% to 5.5% of the adventitia volume, using initialization of every 50th image. An example is shown in Figure 7.

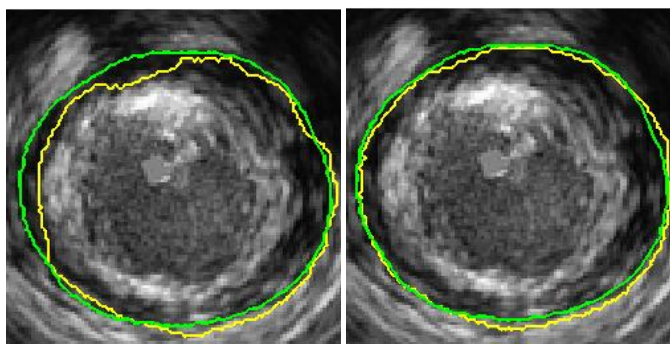


Fig. 7. (a) Adventitia contour found with the non-directional speed term (inner contour, yellow) and the ground truth contour (outer contour, green); (b) adventitia contour found with the new directional gradient speed term (yellow) and the ground truth contour (green)

The final test in this research was to evaluate the benefit of post processing the results from the fast marching method with the level set method, versus using the fast marching method alone. For the weighting coefficients, we empirically chose the following values for β and ϵ : 0.15 and 0.1 for the lumen contour, and 0.1 and 0.15 for the adventitia contour.

The two approaches were applied to the lumen and adventitia contours of dataset #1, and the lumen contour of dataset #2. In both approaches, the datasets were motion corrected and the directional gradient speed term was used. Use of the level-set technique lowered the non-overlapping volume from 7.6% to 5.9% of the lumen volume and 5.5% to 4.5% of the adventitia volume for the first dataset, and 6.0% to 4.7% of the lumen volume for the second dataset.

The 3D level-set method reduced the percentage of non-overlapping area between the segmented area and the ground truth area for almost every image. Figure 8 shows a plot of the error for each image of dataset #1.

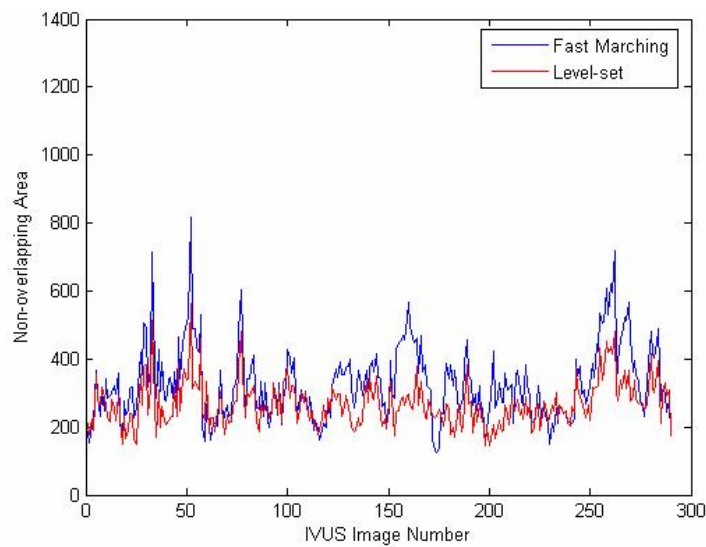


Fig. 8. The error in lumen area (pixels) for the solution from the 3D fast marching method (blue) and the post-fast marching level-set (red) for the adventitia of dataset #1

The power of the level-set method to obtain a smooth curvature while also seeking edges was not as necessary after the new directional gradient term was used in the 3D fast marching method. The directional gradient term eliminated most of the curvature errors that occurred with the non-directional gradient speed term, and found solutions close to the desired edge. Improvements with the level-set technique were small in the two datasets, but did obtain more satisfactory solutions.

4 Conclusion

We have shown three techniques to improve segmentation of IVUS data over existing methods published in the literature. These improvements were shown to more accurately determine the lumen and adventitia volume on IVUS datasets.

A disadvantage in the segmentation method described in this research is that an initial guess must be provided. A fully automated and accurate IVUS segmentation

would be the ideal method. This would require automated initialization of the fast marching method.

Further investigation into the three techniques used in this research might lead to improved segmentation. The parameters of the Gaussian filter used for the velocity term in both the fast marching and level-set method could be studied. These are important because the gradient edges, created with the Gaussian filter, drive both segmentation methods. Another important aspect that could be further investigated is the coefficients used in the level-set equation. It has been widely reported that the lumen geometry can be oddly shaped and patient specific. The curvature term on the level-set method needs to allow the freedom of the level-set to deform to such geometries, but still maintain a reasonable curvature constraint.

Lastly, further testing should be done on a large number of datasets to fully evaluate the algorithm. The datasets should contain vessels with various levels of atherosclerotic plaque as well as vessels that contain stents.

References

1. Klingensmith, J., Shekhar, R., Vince, D.G.: Evaluation of Three-Dimensional Segmentation Algorithms for the Identification of Luminal and Medial-Adventitial Borders in Intravascular Ultrasound Images. *IEEE Transactions on Medical Imaging* 19(10), 996–1011 (2000)
2. Klingensmith, J., et al.: Validation of an Automated System for Luminal and Medial-Adventitial Borders Detection in Three Dimensional Intravascular Ultrasound. *Int'l J. of Cardiovascular Imaging* 19(2), 93–104 (2003)
3. Kovalski, G., Beyar, R., Shofti, R., Azhari, H.: Three-Dimensional Automatic Quantitative Analysis of Intravascular Ultrasound Images. *Ultrasound in Medicine and Biology* 26(4), 527–537 (2000)
4. Shekhar, R., et al.: Three-dimensional Segmentation of Luminal and Adventitial Borders In Serial Intravascular Ultrasound Images. *Computerized Medical Imaging & Graphics* 23(6), 299–309 (1999)
5. Kass, M., Witkin, A., Terzopoulos, D.: Dynamic snakes: Active contour models. *International Journal of Computer Vision* 1(4), 321–331 (1988)
6. Cardinal, M., Meunier, J., Soulez, G., Therasse, E., Cloutier, G.: Intravascular Ultrasound Image Segmentation A Fast-Marching Method. In: Ellis, R.E., Peters, T.M. (eds.) *MICCAI 2003*. LNCS, vol. 2879, pp. 432–439. Springer, Heidelberg (2003)
7. Cardinal, M., Soulez, G., Maurice, R., Therasse, E., Cloutier, G.: Intravascular Ultrasound Image Segmentation: A Three-Dimensional Fast-Marching Method Based on Gray Level Distributions. *IEEE Transactions On Medical Imaging* 25(5), 590–601 (2006)
8. Hernandez, A., Radeva, P., Tovar, A., Gil, D.: Vessel Structures Alignment by Spectral Analysis of IVUS Sequences. In: *The 1st International Workshop on Computer Vision for Intravascular and Intracardiac Imaging*, Copenhagen, Denmark (2006)
9. Sethian, J.: *Level Set Methods and Fast Marching Methods*. Cambridge University Press, New York (1999)
10. Sarti, A., et al.: A Unified Geometric Model for 3D Confocal Image Analysis in Cytology. In: *Proc. of the Int'l Symp. Computer Graphics, Image Processing, and Vision*, p. 69 (1998)
11. Dicker, J.: *Fast Marching Methods and Level Set Methods: An Implementation*. Ph.D. Thesis: University of British Columbia, Okanagan Campus (2006)